Carbohydrate Polymers 372 (2026) 124540

Contents lists available at ScienceDirect

Carbohydrate Polymers

journal homepage: www.elsevier.com/locate/carbpol

Synthesis and characterization of heptakis (methylaminoethanol)-β-cyclodextrin, carvacrol complexation and evaluation of antioxidant, antibacterial and antibiofilm activities

Sonia Pedotti [a,1], Giovanna Ginestra [b,1], Giuseppe Granata [a,1], Loredana Ferreri [a], Giovanni Gambera [a], Salvatore Petralia [a,c], Francesco Ruffino [d,e], Maria Fernanda Taviano [b], Antonia Nostro [b,*], Grazia Maria Letizia Consoli [a,*]

[a] CNR - Institute of Biomolecular Chemistry, Via Paolo Gaifami 18, 95126, Catania, Italy
[b] Department of Chemical, Biological, Pharmaceutical and Environmental Sciences, University of Messina, 98166, Messina, Italy
[c] Department of Drug and Health Sciences, University of Catania, Via Santa Sofia 64, 95125, Catania, Italy
[d] Department of Physics and Astronomy "Ettore Majorana" University of Catania, Via Santa Sofia 64, 95123, Catania, Italy
[e] CNR - Institute for Microelectronics and Microsystems, Via Santa Sofia 64, 95123, Catania, Italy

ARTICLE INFO

Keywords:
Cyclodextrin
Inclusion complex
Nanobiotic
Carvacrol
Antibacterial
Antibiofilm

ABSTRACT

Cyclodextrins are widely explored as drug delivery systems for pharmaceutical applications. Here, we synthesized and characterized a novel β-cyclodextrin derivative functionalized with seven methylaminoethanol groups (βCD-MEA). The functionalization effects on water solubility, self-assembly behavior, toxicity, antibacterial activity, and drug complexation were investigated. Dynamic light scattering and microscopy images revealed βCD-MEA forms water soluble *quasi*-spherical nanoaggregates. Toxicological evaluation on *Artemia salina* indicated no toxicity of βCD-MEA, while antibacterial biofilm assays demonstrated its ability to reduce preformed *Staphylococcus aureus* biofilm. The potential of βCD-MEA as a drug delivery system was assessed using carvacrol as a drug model. The inclusion complex of βCD-MEA and carvacrol was prepared via freeze-drying, and key parameters such as apparent stability constant, complexation efficiency, drug loading capacity, drug entrapment efficiency, and dry content were determined. The size and morphology of the βCD-MEA/Carvacrol nanoaggregates were also examined. The complexed carvacrol retained its radical scavenging activity, exhibited antibacterial effects against *S. aureus* and *Escherichia coli*, and reduced both the formation and the amount of preformed biofilm *S. aureus*. The intrinsic ability of the βCD-MEA nanoaggregates to affect the preformed biofilm of *S. aureus*, combined with its potential as a nanocarrier for drug delivery, suggest βCD-MEA as a promising novel candidate in nanobiotics.

1. Introduction

Cyclodextrins (CDs) are a family of macrocyclic oligomers composed of D-(+)-glucopyranosyl units linked by α-1,4-glycosidic bonds (6, 7, and 8 glucose units for α-, β-, and γ- cyclodextrins, respectively). The chair conformation of the glucose units generates a truncated cone-like shape with a hydrophobic cavity resulting from the methylene and oxygen groups, and a hydrophilic external surface formed by primary and secondary hydroxyl groups. The presence of the hydrophobic cavity, which can host a variety of bioactive molecules (Esteso & Romero, 2024), has led to the use of cyclodextrins and some of their derivatives as FDA-approved additives in the food industry (Pollit, 1996). Inclusion within the cyclodextrin cavity can enhance the water solubility, dissolution rate, stability, and bioavailability of poorly water-soluble drugs (Singh & Mahar, 2024). Currently, more than 100 approved pharmaceutical ingredients are formulated using native cyclodextrins or their derivatives as excipients (Puskás et al., 2023). Recently, cyclodextrins have also been explored as active ingredients for the treatment of various diseases. They can prevent accumulation and counteract direct harmful interactions of target compounds with tissues, and modulate

* Corresponding authors.
E-mail addresses: antonia.nostro@unime.it (A. Nostro), graziamarialetizia.consoli@cnr.it (G.M.L. Consoli).
[1] These authors equally contributed.

https://doi.org/10.1016/j.carbpol.2025.124540
Received 23 July 2025; Received in revised form 12 October 2025; Accepted 13 October 2025
Available online 19 October 2025

their pharmacokinetics (Kfoury et al., 2025).

Among cyclodextrins, β-cyclodextrin (β-CD) is the most commercially available oligomer, accounting for approximately 70 % of global cyclodextrins production, with applications spanning material science, food, and pharmaceuticals (Fatima et al., 2023; Gonzalez Pereira et al., 2021). β-CD exhibits poor water solubility due to strong intramolecular hydrogen bonding among its secondary hydroxyl groups (French et al., 1949). In contrast, the primary hydroxyl groups, being less hindered and more nucleophilic, are easily functionalized to tailor physiochemical properties and guest complexation behavior (Hbaieb et al., 2008; Huang et al., 2024). Recently, our group developed β-cyclodextrin-derived carbon nanodots and demonstrated their photothermal properties (Maugeri et al., 2025) as well as their ability to form complexes with bioactive molecules such as curcumin, ciprofloxacin and carvacrol (Consoli et al., 2025).

Amino alcohols are important subunits, that establish hydrogen bonding and ionic interactions in molecular recognition events. They are commonly found in natural products (e.g., alkaloids and antibiotics), biologically active molecules, (e.g. adrenaline, sphingosine, propanolol), and ligands for cell receptor recognition. For example, choline and ethanolamine serve as ligands for crossing biological barriers (Granata et al., 2017) and targeting cancerous and bacterial cells by binding choline transporters (Neves et al., 2022; Ri et al., 2024; Watanabe et al., 2020).

To the best of our knowledge, there are few reports in the literature describing β-cyclodextrins functionalized with β-amino alcohol moieties (Martina et al., 2011). These include derivatives that exhibit enzyme-mimetic activity (Shen & Ji, 2012) or iodophor and mucoadhesive behavior (Pedotti et al., 2024).

We hypothesized that introducing seven polar methylaminoethanol groups to the primary hydroxyls of the β-CD backbone could provide a novel β-CD derivative (βCD-MEA) that might combines the drug complexing ability of the β-CD cavity with the ligand properties of β-amino alcohol groups, and might self-assemble in water-soluble nanoaggregates. Therefore, βCD-MEA could contribute to the search for novel β-cyclodextrin-based drug delivery systems that could harness the advantages of nanotechnology.

To experimentally confirm these hypotheses, here we performed: (i) the synthesis of βCD-MEA; (ii) its characterization by Nuclear Magnetic Resonance (NMR) spectroscopy, Electrospray Ionization Mass Spectrometry (ESI-MS), Fourier Transform Infrared Spectroscopy (FT-IR), (iii) the evaluation of its self-assembly in nanostructures by Dynamic Light Scattering (DLS), Electrophoretic Light Scattering (ELS), and Atomic Force Microscopy (AFM); (iv) the assessment of βCD-MEA potential toxicity using the *Artemia salina* lethality assay; (v) the investigation of the capability of βCD-MEA to complex carvacrol (CAR), selected as a model drug with known antioxidant and antibacterial properties (Sharifi-Rad et al., 2018), but affected by poor water solubility, low chemical stability, high volatility, and intense flavor that can compromise the organoleptic properties of pharmaceutical products; (vi) the characterization of the inclusion complex in terms of stoichiometry, apparent stability constant, and complexation efficiency; (vii) the investigation of the structure of the βCD-MEA/carvacrol complex via molecular modelling simulations; (viii) the assessment of the antioxidant activity of the complex using the DPPH radical scavenging assay; (ix) the evaluation of the antibacterial activity of both βCD-MEA and βCD-MEA/CAR complex against Gram-positive (*Staphylococcus aureus*) and Gram-negative (*Escherichia coli*) bacteria, along with an analysis of their effects on *S. aureus* biofilm in comparison with CAR alone.

Overall, the conducted experiments led us to ascertain the ability of the designed βCD-MEA to act as a water-soluble nanosized container capable of hosting carvacrol within the cyclodextrin cavity and exhibit radical scavenging, antibacterial and antibiofilm activities.

2. Material and methods

2.1. Materials

All chemicals, including heptakis(6-iodo-6-deoxy)-β-cyclodextrin precursor, were obtained from commercial sources (Sigma-Aldrich, Milan, Italy) and used without further purification.

2.2. Instrumentation

Freeze-drying was performed on a LyoQue\1st-85 (Telstar, Italy) freeze dryer. NMR spectra were recorded on a Bruker 400™ spectrometer (Bruker, Germany), chemical shift (δ) are reported in parts per million (ppm) referring to the residual solvent signal (HOD, 4.7 ppm). 2D-ROESY NMR experiments were acquired with a mixing time of 300 ms. ESI-MS spectra were acquired on a Orbitrap Exploris 120 (Thermo Scientific, USA) instrument. ATR-FTIR spectra were acquired on a Perkin-Elmer Spectrum Two Fourier Transform Infrared spectrophotometer with attenuated total reflectance modules (Perkin-Elmer, Long Island, NY, USA). Atomic Force Microscopy (AFM) analyses were performed using a Bruker-Innova microscope operating in high amplitude mode and ultra sharpened Si tips, MSNL-10 from Bruker Instruments (Karlsruhe, Germany), with anisotropic geometry, radius of curvature 2 nm, tip height 2.5 nm, front angle 15°, back angle 25°, side angle 22.5°, resonance frequencies of 90–160 kHz, nominal spring constant of 0.07 N/m were used and substituted as soon as a loose resolution was observed during the acquisition. AFM images were reconstructed by acquiring 512 × 512 lines, scan rate 0.8 Hz, and were analyzed by using the SPMLABANALYSES V7.00 software. DLS and ELS measurements were performed on a ZetaSizer NanoZS90 (Malvern Instrument, Malvern, UK) equipped with a 633 nm laser, at the scattering angle of 90° and 25 °C temperature. HPLC analyses were performed on a Dionex HPLC system (P680 pump, ASI-100 autosampler, UVD170U detector, TCC-100 temperature-controlled column compartment).

2.3. Methods

2.3.1. Synthesis and characterization of heptakis-(6-methylaminoethanol-6-deoxy)-β-CD (βCD-MEA)

Commercial heptakis(6-iodo-6-deoxy)-β-cyclodextrin (0.1 g, 0.053 mmol) was dissolved in neat *N*-methylethanol amine (0.5 mL, 6.22 mmol) and the mixture reaction was stirred at 70 °C for 20 h under argon atmosphere. The solvent was evaporated to dryness in vacuo. The crude mixture was purified by reversed-phase chromatography (LiChroprep RP18) (eluent: H_2O:CH_3OH; 100:0–0:100, *v/v*). The final product was recovered with approximately 50 % water/methanol (*v/v*) as the eluent. The eluate was dried in vacuo. Finally, the solid was disperded in water and freeze-dried to give a white solid in 80 % yield (0.065 g, 0.042 mmol); Rf: 0.55 (Propanol/H_2O/NH_4OH/AcOEt, 5:3:2:1, *v/v/v/v*); $[\alpha]_D^{25} = +100$ (H_2O).

The final product was characterized by NMR spectroscopy and ESI HR-MS spectrometry. ^{1}H NMR (400.13 MHz, D_2O, 297 K): $\delta = 5.14$ (d, $J = 3$ Hz, 7H, H-1), 3.85 (m, 14 H, H-3 and H-5), 3.61 (m, 14H, CH_2O), 3.47 and 3.42 (dd, $J = 3.2$ Hz, $J = 10.1$ Hz, 14 H, H-2 and H-4), 2.73 (m, 14H, H-6), 2.56 (m, 14 H, CH_2N), 2.24 (s, 21H, CH_3N); ^{13}C NMR (100.62 MHz, D_2O, 297 K): $\delta = 99.1$ (C-1), 79.9 (C-4), 72.6 (C-3), 71.6 (C-2), 69.2 (C-5), 59.3 (CH_2O), 58.2 (C-6), 57.2 (CH_2N), 42.5 (CH_3N).

The sample for ESI HR-MS analysis (1×10^{-5} M concentration) was prepared by dispersing βCD-MEA in a water/methanol mixture (9:1, *v/v*). The sample was injected at a flow rate of 50 μL/min. Vaporizer Temperature (VT) = 290 °C, Ion Transfer tube Temperature (ITT) = 290 °C, optimum Sheath Gas Pressure (SGP) = 35 psig, Auxiliary Gas Pressure (AGP) = 5 psig, Ion Spray Volt (ISV) = 3200 V and positive mode. ESI HR-MS spectrum: calculated for $C_{63}H_{119}N_7O_{35}$ *m/z* 1533.77; found *m/z* 767.88 $[M + 2H]^{2+}$, 512.26 $[M + 3H]^{3+}$, and 384.44 $[M + 4H]^{4+}$. Smaller peaks at *m/z* 730.35 $[M + 2H\text{-MEA}]^{2+}$, 487.23 [M + 3H-

MEA]$^{3+}$, and 365.68 [M + 4H-MEA]$^{4+}$ consistent with a hexa-substituted derivative were also detected. Aliquots of the lyophilized powder of βCD-MEA were dispersed in water for biological assays.

2.3.2. DLS, ELS, and AFM analyses of βCD-MEA

βCD-MEA (5 mg) was dispersed in 1.2 mL pure water and the sample was passed through a 0.45 μm RC filter. Size (Z average), polydispersity index (PDI) and size distribution were determined by DLS experiments, whereas Zeta potential value and Zeta potential distribution by ELS measurements.

For AFM analysis, water dispersions of βCD-MEA (1 mg/mL or 5 mg/mL) were passed through a RC filter (0.45 μm pore size) and an aliquot (50 μL) of each sample was dispensed on Silicon substrates and dried. Samples were prepared by drop casting onto pre-cleaned silicon substrate and were allowed to dry under gentle nitrogen blow-drying to ensure proper adsorption.

2.3.3. Artemia salina lethality bioassay

The potential toxicity of βCD-MEA was preliminarily assessed by the brine shrimp (*Artemia salina* Leach) lethality bioassay, according to a method reported in the literature (Meyer et al., 1982) with some modifications. Brine shrimp eggs were hatched in artificial seawater (32 g/L sea salt in distilled water) by incubation under a 60 W lamp, at a temperature of 24–26 °C. After 24 h incubation, hatched nauplii were collected and further incubated for 24 h in artificial seawater in the same condition. For the assay, serial dilutions of βCD-MEA in distilled water were prepared. Ten brine shrimp larvae were transferred in petri dishes filled with artificial seawater mixed with 375 μL of each sample dilution, to obtain the final concentrations 1.75, 0.87, and 0.44 mg/mL in a volume of 1.5 mL, and incubated at 24–26 °C under continuous lighting for 24 h. At the time point, the surviving larvae were counted using a magnifying glass and median lethal concentration (LC_{50}) value was determined. Control groups were prepared for seawater and seawater with 375 μL mL distilled water. For each sample concentration and the controls, three replicates were used. The toxicity level of the extract was assessed based on Clarkson's toxicity scale (Hamidi et al., 2014).

2.3.4. Preparation of βCD-MEA/CAR inclusion complex

βCD-MEA/CAR inclusion complex was prepared by freeze-drying method. Carvacrol (1.8 μL, 11.7 μmol) was dispersed in a sample of βCD-MEA (10 mg, 6.5 μmol, in 10 mL water). The mixture was magnetically stirred at room temperature for 24 h in the dark. As a control, CAR alone (1.8 μL) was dispersed in water (10 mL) and magnetically stirred at the same conditions. The resulting dispersions were freeze-dried for 48 h. Aliquots of the lyophilized powder of βCD-MEA/CAR were dispersed in water for biological assays.

2.3.5. Determination of drug loading capacity (%),entrapment efficiency (%), and dry content (%)

The amounts of CAR alone and in the complex with βCD-MEA were determined by HPLC using a Phenomenex Luna Omega 5 μm C18 reverse-phase column (150 × 4.6 mm) and 2.5 % formic acid (*v*/v) in water:acetonitrile (60:40 %, *v/v*) as the mobile phase (flow rate 1.0 mL/min, $T = 25$ °C). The amounts of CAR were determined from the peak at $\lambda = 274$ nm by referring to a calibration line plot. Drug loading capacity (%) and drug encapsulation efficiency (%) were determined by the following equations:

$$Drug\ loading\ capacity\ (\%) = \frac{CAR\ in}{\beta CD - MEA + CAR\ in} \times 100 \quad (1)$$

where "*CAR in*" is the mass of carvacrol in the lyophilized complex and "*βCD-MEA + CAR in*" is the sum of the mass of βCD-MEA and the mass of CAR in the lyophilized complex.

$$Entrapment\ Efficiency\ (\%) = \frac{CAR\ in}{CAR\ initial} \times 100 \quad (2)$$

where "*CAR in*" is the mass of carvacrol in the lyophilized complex and "*CAR initial*" is the mass of CAR added to the βCD-MEA nanosuspension before the freeze-drying process.

The dry content (%) of the βCD-MEA/CAR complex was calculated for a nanosuspension containing 5 mg of βCD-MEA and 750 μg of carvacrol in 1.2 mL water. An aliquot of nanosuspension (396 mg) was kept at 105 °C for 24 h.

$$Dry\ Content\ (\%) = \frac{W3 - W1}{W2 - W1} \times 100$$

$W1$ = weight of empty container
$W2$ = weight of nanosuspension
$W3$ = weight of solid residue

2.3.6. DLS, ELS, and AFM analyses of the βCD-MEA/CAR complex

DLS and ELS experiments were performed on a nanosuspension of βCD-MEA/CAR complex, containing 5 mg βCD-MEA in 1.2 mL water and passed through a Sartorius RC filter (0.45 μm pore size) to ensure the accuracy, reliability, and reproducibility of the measurements.

For AFM analysis, water dispersions of βCD-MEA/CAR (βCD-MEA 1 mg or 5 mg/mL) were passed through a RC filter (0.45 μm pore size) and an aliquot (50 μL) of each sample was dispensed on Silicon substrates and dried. Samples were prepared by drop casting onto pre-cleaned silicon substrate and were allowed to dry under gentle nitrogen blow-drying to ensure proper adsorption.

2.3.7. Phase solubility study

Phase solubility experiments were carried out as described by Higuchi and Connors (Higuchi & Connors, 1965). An excess of CAR (2 μL, 13 μmol) was added to 0.5 mL of βCD-MEA at concentrations ranging from 0 to 6 mM. The samples were placed at 25 °C in a laboratory shaker for 24 h. Then, they were passed through 0.45 μm RC Sartorius filters and the quantity of carvacrol was determined by HPLC analysis (see *2.3.3.*). Stability constant (K_c), complexation efficiency (*CE*) and CAR solubility enhancement factor (δ) were calculated according to the following equations:

$$K_c = \frac{Slope}{S_0\,(1 - Slope)} \quad (3)$$

$$CE = \frac{Slope}{1 - Slope} \quad (4)$$

2.3.8. Molecular modelling simulations

Computational calculations were performed with the software xtb (extended Tight Binding, version 6.6.1). A rough inclusion complex was obtained by manually including carvacrol into optimized βCD-MEA. The structures of βCD-MEA and rough βCD-MEA/CAR inclusion complex were optimized with the GFN2-xTB method, to a very-tight level (−-opt vtight) and with implicit water (−-alpb water). To find the lowest energy conformer, the xTB-optimized inclusion complex was submitted to the xtb utility CREST (Conformer-Rotamer Ensemble Sampling Tool) in the NCI (Non-Covalent Interaction) option and with implicit water (Plett & Grimme, 2023). Analysis of interatomic distances was executed with Mercury (2024.3.1-build 428097- Copyright© CCDC, 2021–2024).

2.3.9. Antioxidant assay

The free radical scavenging activities of βCD-MEA, βCD-MEA/CAR and CAR alone were estimated by using the 2,2-diphenyl-1-picrylhydrazyl (DPPH) assay, adapting a protocol previously described by Ohnishi and coworkers (Ohnishi et al., 1994) with modifications. For each sample, serial dilutions with distilled water (1:2) were prepared. CAR was preliminarily tested at concentrations ranging from 800 to 12.5 μg/mL; then, βCD-MEA (1.34–0.08 mg/mL) alone and loaded with CAR (200–12.5 μg/mL) were assayed. Briefly, a 28.6 μL aliquot of each sample was dispensed into a 96-well microplate holding 171.4 μL of

freshly prepared DPPH methanol solution (0.1 mM), with a final volume in each well up to 200 µL. The reaction mixture was incubated under stirring on an orbital shaker (50 rpm) at room temperature and in the dark for 20 min; at the time point, absorbance was measured at 517 nm against the corresponding blank using a UV–Vis reader plate (Multiskan GO; Thermo Scientific, Waltham, MA, USA). The scavenging activity was measured as the decrease in absorbance of the samples versus the DPPH standard solution. The results were obtained from the average of three independent experiments and are reported as mean radical scavenging activity percentage (%) ± standard deviation (SD).

2.4. Microbiological studies

2.4.1. Minimal inhibitory concentration and minimal bactericidal concentration

The bacteria used in this study were: *Staphylococcus aureus* (ATCC 6538) and *Escherichia coli* (ATCC 10536). Minimal Inhibitory Concentration (MIC) and Minimal Bactericidal Concentration (MBC) of βCD-MEA/CAR (1.34 mg/mL and 200 µg/mL), CAR (200 µg/mL) and βCD-MEA (1.34 mg/mL) samples, were performed according to the guidelines of the Clinical and Laboratory Standards Institute (CLSI, 2018), with some modifications. The samples were two-fold diluted in 96-well round-bottomed using Mueller-Hinton Broth (MHB) and overnight bacterial cultures were inoculated to yield a final concentration of 5×10^5 CFU/mL. The MIC was considered as the lowest concentration of sample giving the inhibition of visible bacterial growth after incubation for 24 h. The MBC was determined by seeding 20 µL from all clear wells onto Muller Hinton agar and incubated at 37 °C for 24 to 48 h. The MBC was defined as the lowest concentration killing 99.9 % of the inoculum. The data from at least three replicates were evaluated, and modal results were calculated.

2.4.2. Effect on biofilm formation

Effect of βCD-MEA/CAR, CAR, and βCD-MEA on biofilm formation was estimated as previously reported (Nostro et al., 2007). Overnight culture of *S. aureus* (ATCC 6538) in TSB + 1 % glucose (TSBG) was adjusted to 1×10^6 CFU/mL and 1 mL of standardized culture was added individually to each well of a 96-well cell culture treated polystyrene microtiter plate containing βCD-MEA/CAR, CAR and βCD-MEA. Controls consisting of Tryptic Soy Broth (TSBG) with and without *S. aureus* addition were included. The plates were incubated at 37 °C for 24 h, then the effect on biofilm formation was evaluated as follows: the biofilm biomass formed in each well was washed twice with PBS, dried, stained for 1 min with 0.1 % safranin, and then washed with water as previously reported (Nostro et al., 2007). The stained biofilms were resuspended in 30 % (*v*/v) acetic acid and optical density (OD_{492}) was measured using a spectrophotometer EIA reader (Bio-Rad Model 2550). The reduction percentage of biofilm biomass was calculated using the following equation:

$$Biofilm\,Reduction\,(\%) = 100 - \left(\frac{OD\ control - OD\ sample}{OD\ control} \times 100\right) \quad (6)$$

2.4.3. Effect on preformed biofilm

Effect of βCD-MEA, βCD-MEA/CAR, and CAR on preformed biofilm was estimated as previously reported (Nostro et al., 2009). Overnight culture of *S. aureus* ATCC 6538 grown in TSBG was standardized to 1×10^6 CFU/mL and was inoculated (100 µL) in 96-well polystyrene flat-bottomed microtiter plates. After incubation for 24 h at 37 °C, the planktonic bacterial growth was dislodged and the wells were washed with sterile PBS and filled with two-fold dilutions of samples, ranging from 0.5 × MIC to a 4-fold MIC (referred to the values reported in Table 1). After incubation for 24 h at 37 °C, the planktonic growth was dislodged and each well was washed with PBS, dried, stained with 0.1 % safranin and then washed with water. The biofilm biomass was eluted in acetic acid 30 % (*v*/v) and the OD_{492} was quantified. The reduction of biofilm biomass was estimated using the above reported Eq. (6).

Table 1
Antibacterial activity of βCD-MEA/CAR, CAR, and empty βCD-MEA.

Strains	βCD-MEA/CAR	CAR	βCD-MEA
	MIC (mg/mL)		
S. aureus ATCC 6538	0.05	0.05	>0.67
E. coli ATCC 10536	0.1	0.1	>0.67

2.4.4. Statistical analysis

Results were expressed as the mean value ± standard deviation from three experiments. An analysis of variance (ANOVA) was used to determine significant differences between groups treated with βCD-MEA/CAR and CAR. Where significant differences existed, the Duncan test was performed to verify the significant difference levels. The results with a p-value <0.05 were considered statistically significant.

3. Results and discussion

3.1. Synthesis and structural characterization of heptakis-(6-methylaminoethanol-6-deoxy)-β-CD (βCD-MEA)

To tether methylaminoethanol moieties to the primary hydroxyls of β-cyclodextrin, we envisioned a simple nucleophilic substitution reaction using commercially available heptakis(6-iodo-6-deoxy)-β-cyclodextrin as the precursor. Briefly, the precursor was stirred with an excess of *N*-methylethanolamine to give heptakis-(6-methylaminoethanol-6-deoxy)-β-cyclodextrin (βCD-MEA) with 80 % yield (Fig. 1).

The formation of βCD-MEA was investigated by 1D- and 2D-NMR, ESI-MS, and FT-IR techniques. ^{1}H NMR (Fig. S1), ^{13}C- and DEPT-NMR spectra (Figs. S2-S3) of βCD-MEA showed the typical signals of the cyclodextrin scaffold and additional signals relative to the substituent moieties. The NMR signal pattern agreed with a fully symmetric structure consistent with an exhaustive functionalization of the cyclodextrin methylene groups in position 6 of the glucose units. Proton signals at 2.24, 2.56, and 3.61 ppm, and carbon signals at 42.5, 57.2, and 59.3 ppm, were observed for N-CH_3, N-CH_2 and CH_2O protons of the substituent groups, respectively. The NMR assignment of the βCD-MEA resonances was supported by 2D-NMR spectra (Figs. S4-S6).

The functionalization of the methylene groups on the βCD backbone was confirmed by the ESI-MS spectrum, which showed pseudomolecular ion peaks with doubly (m/z 767.88), triply (m/z 512.26), and quadruply (m/z 384.44) charged species. The spectrum also displayed smaller multicharged ion peaks, consistent with the presence of a hexa-substituted derivative (Fig. S7). The low amount of hexa-substituted derivative in the sample was supported by the NMR spectra, which, within the 5 % error margin of the technique, showed only a single set of signals consistent with a symmetrical and fully substituted cyclodextrin (Figs. S1–S2).

Further evidence of βCD functionalization was provided by the ATR-FTIR spectrum of βCD-MEA, which showed a shift in the OH stretching peak from 3300 to 3289.4 cm^{-1} (Fig. S8).

3.1.1. Self-aggregation of βCD-MEA and morphological analysis of the water-soluble nanoaggregates

Dipole interactions between the hydrophilic outer edges and bulk water molecules allow for the dissolution of cyclodextrins in water. Nevertheless, β-CD has been reported to have low solubility (18.5 mg/mL at 25 °C) and a high tendency to self-aggregate in water (Dodziuk, 2006). Aggregation phenomena were observed for β-CD at 2–3 mM concentrations using dynamic and static light scattering measurements; cryo-TEM images revealed the presence of quasi-spherical polydisperse objects with diameters of about 100 nm at lower β-CD concentrations and micrometer-sized planar aggregates as the predominant population

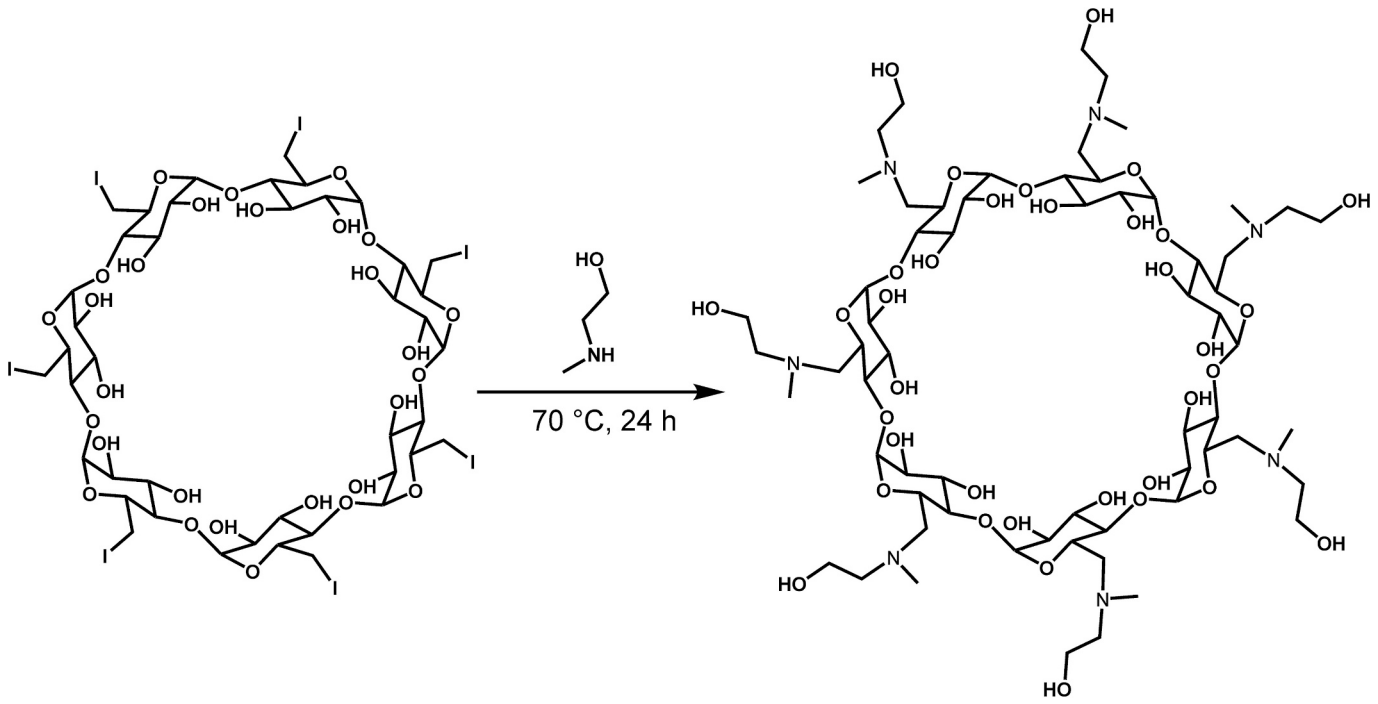

Fig. 1. Synthetic procedure for the preparation of βCD-MEA starting from the commercial heptakis(6-iodo-6-deoxy)-β-cyclodextrin precursor.

at higher concentrations (Bonini et al., 2006).

Several works reported that the functionalization of the βCD skeleton, by disrupting intramolecular hydrogen bonding, can provide βCD derivatives with water solubility higher than the precursor. In agreement, the water solubility of βCD-MEA compared to the native βCD increased from 18.5 mg/mL to at least 100 mg/mL.

The dispersion of βCD-MEA in water provided a clear and transparent nanosuspension as evidenced by DLS measurements that showed the presence of water soluble nanoaggregates (Fig. 2A) with mean hydrodynamic diameter of 248 ± 1 nm (Z average). Polydispersity index (PDI), that measures the uniformity of the particle sizes, was found to be 0.19 ± 0.01 indicative of a narrow uniform size distribution, suitable for drug delivery application. Electrophoretic light scattering (ELS) measurements provided a negative Zeta potential value (ζ = −46 ± 1 mV) for the nanoaggregates present in the nanosuspension (Fig. 2B).

AFM images evidenced that βCD-MEA (1 mg/mL) forms quasi-spherical shaped nanoaggregates with average height of 39.5 ± 14.7 nm and average width of 108.6 ± 27.2 nm (Fig. 2C). The flattening of the nanoaggregates can be due to the pressure during AFM analysis and can be indicative of their deformability, an important requisite for

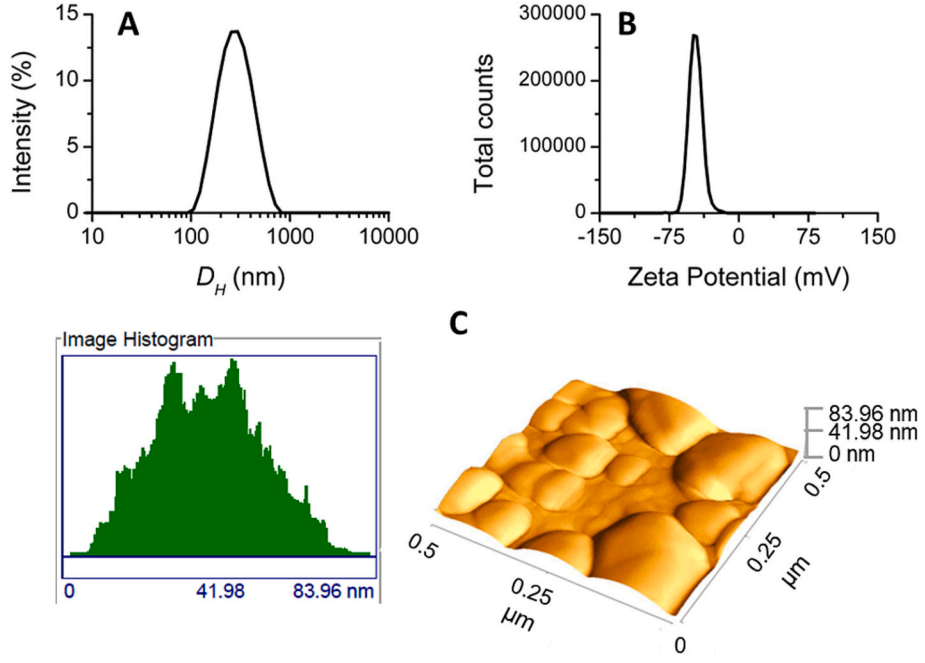

Fig. 2. Characterization of βCD-MEA nanoaggregates: A) Intensity weighted distribution of the mean hydrodynamic diameter; B) Zeta potential distribution; C) Size distribution histogram and representative AFM image of βCD-MEA nanoaggregates (1 mg/mL in water) on Si substrate.

penetration through tissue fenestrations in the body (Granata et al., 2025). Morphology and size of the nanoaggregates was maintained at higher βCD-MEA concentration (5 mg/mL, 53.5 ± 17.6 nm average height and 100.6 ± 29.1 nm average width, Fig. S9).

3.1.2. *Preliminary assessment of βCD-MEA toxicity*

For a potential application of βCD-MEA as a nanocarrier for bioactive compounds, we investigated its toxicity. *Artemia salina* Leach (Artemiidae), commonly known as brine shrimp, is a microcrustacean which thrives in extremely saline environments and is used for a preliminary and rapid toxicity screening of synthetic and natural products (Yu & Lu, 2018). The advantages of using *A. salina* include high sensitivity, cost-effective culture requirements, relatively ease of maintenance under laboratory conditions, and rapid test results (Libralato et al., 2016). Based on the Clarkson's toxicity scale, LC_{50} values greater than 1000 μg/mL indicate absence of toxicity (Hamidi et al., 2014).

The results of the bioassay carried out for the βCD-MEA demonstrated the lack of toxicity toward brine shrimp larvae; indeed, 100 % survival rate was observed at all tested concentrations, with a LC_{50} value above 1.75 mg/mL, which indicates the potential safety of the system.

3.2. *Preparation and characterization of βCD-MEA/Carvacrol complex*

Several parameters influence the complexation behavior of cyclodextrins, including the type of functional groups introduced into the cyclodextrin scaffold and the charge and hydrophobicity of the guest. To evaluate whether the amino-alcohol groups decorating the cavity of βCD-MEA influence the complexing properties of the βCD macrocycle, CAR was chosen as a model of hydrophobic, volatile and multifunctional drug, whose possibility to be included in the cavity of β-cyclodextrins has been reported (Ates & Yildiz, 2025; Rodríguez-López et al., 2020).

The βCD-MEA/CAR complex was prepared by freeze-drying technology (Li et al., 2022), that is the method mostly used in the manufacturing of biopharmaceutical products allowing for better handling, dosing, and stability. The amount of CAR in the lyophilized complex, after dispersion in water, was determined to be 150 μg *per* mg of βCD-MEA, corresponding to a drug loading capacity of 13 % and an encapsulation efficiency of 85 %. Due to its volatility, the amount of CAR in the sample lyophilized without βCD-MEA was only 0.5 μg/mL. This amount, 300-fold lower than that measured in the presence of βCD-MEA, further confirmed the formation of the inclusion complex. The dry content (%) was calculated to be 0.4 % for both filtered and non-filtered samples of βCD-MEA/CAR. A low dry content is often indicative of a more stable colloidal dispersion, with less aggregation or sedimentation phenomena.

3.2.1. *Characterization of the complex by NMR and ATR-FTIR spectroscopy*

Mono- and bi-dimensional NMR experiments evidenced the formation of the βCD-MEA/CAR inclusion complex. Chemical shift variations of both host and guest proton signals were observed in the ^{1}H NMR spectrum (Fig. 3, Table S1). Upfield shift (shielding) was detected for H2 and H4 aromatic protons of CAR (Δδ 0.05 ppm) and for H3 and H5 protons of βCD-MEA (Δδ 0.1 ppm), which are located inside the cyclodextrin cavity and are affected by the proximity of the CAR aromatic rings.

Upfield shift was also observed for the protons of the amino-alcohol groups: N-CH_3, N-CH_2, CH_2O (Δδ 0.06, 0.02, and 0.03 ppm, respectively), suggesting their involvement in the interaction with CAR or a rearrangement of these groups in the complex compared to the empty βCD-MEA. In line with previous reports on βCD/CAR complexes (Locci et al., 2004), downfield shift was instead observed for the isopropyl-CH_3 (H-3″) and CH_3 (H-6′) protons of CAR (Δδ 0.06 and 0.02 ppm, respectively).

The formation of an inclusion complex was corroborated by 2D-ROESY NMR spectra which showed correlation cross-peaks between aromatic H2 and H4 protons of CAR and H3 and H5 protons of βCD-MEA, located inside the hydrophobic cavity. Additional cross-peaks between isopropyl CH_3 (H-3″) of CAR and H3, H5, H6, and N-CH_3 protons of βCD-MEA supported a preferential orientation in which the isopropyl group of CAR is directed toward the narrow edge of the cyclodextrin.

ATR-FTIR spectra also corroborated the formation of the βCD-MEA/CAR complex (Fig. S8). Compared to the spectrum of βCD-MEA alone,

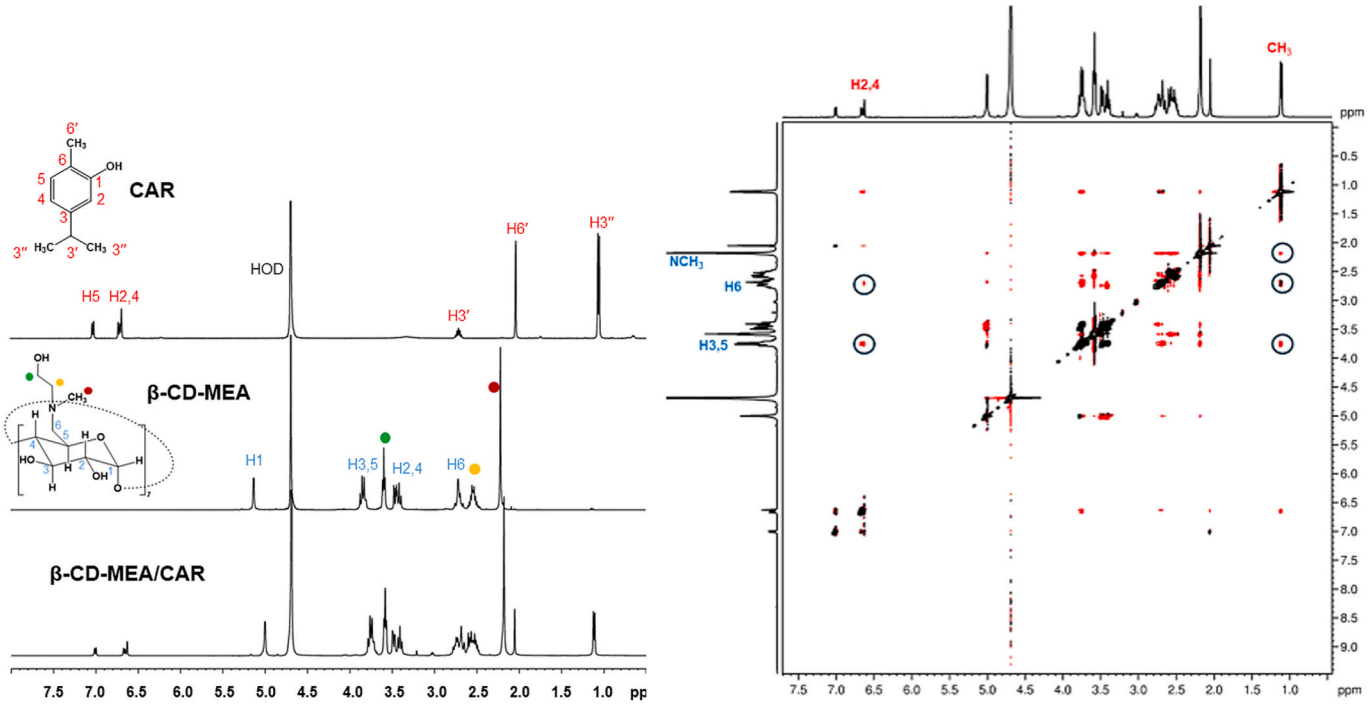

Fig. 3. ^{1}H NMR spectra of CAR (up), βCD-MEA (medium) and βCD-MEA/CAR (bottom), and 2D-ROESY NMR spectrum of the βCD-MEA/CAR complex (400.13 MHz, D_2O, 297 K). The most diagnostic correlation cross-peaks are circled.

the complex displayed the diagnostic peaks of CAR at 3282.6, 2953, 1257.9, and 1178.3 cm^{-1} corresponding to OH stretching, C—H stretching from isopropyl and methyl groups, C—O stretching, and aromatic CH bending, respectively. Shift of these peaks compared to those of CAR alone (3378, 2954, 1251, 1173 cm^{-1}) (Valderrama & Rojas De, 2017), confirmed a complexation rather than a simple physical mixing process.

3.2.2. Molecular modelling simulations

To better insight the geometry of the complex, molecular modelling simulations were carried out. A simulated inclusion complex was optimized with GFN2-xTB and then submitted to CREST (Conformer-Rotamer Sampling Tool) to find the lowest energy conformer (Plett & Grimme, 2023).

The structure in Fig. 4, in which CAR is included into the βCD-MEA cavity with the isopropyl group pointing toward the narrow edge, was found as the lowest energy conformer (−391.31212 Eh). In this structure, the distances between CAR and βCD-MEA atoms involved in the interactions were consistent with the ROE cross peaks, falling within 2.26–4.93 Å range (Fig. S10).

A similar geometry, in which the isopropyl group of CAR enters the βCD-MEA cavity from the wider edge and points toward the narrower edge, has been reported for the inclusion complex of the native βCD with CAR. This orientation was found to be more stable, by circa 3.0 kJ mol^{-1}, than the structure with the isopropyl group directed toward the wider edge of βCD (Cedillo-Flores et al., 2022).

The outer position of the CAR hydroxyl group, involved in the reaction with radical species, is expected to maintain the antioxidant activity of CAR in the βCD-MEA complex.

3.2.3. Phase solubility study

Phase solubility studies are commonly employed to evaluate the ability of cyclodextrins to enhance the aqueous solubility of hydrophobic molecules and determine the apparent stability constant (K_c), which reflects a combination of multiple factors: strength of host–guest interactions, stability of inclusion complexes, self-association of poorly soluble guests, complex aggregation, non-inclusion interactions, and micelle formation (Loftsson et al., 2007).

A phase solubility study showed that the aqueous solubility of CAR increased linearly with increasing βCD-MEA concentration. The phase solubility diagram showed an AL-type profile (Fig. S11), whose slope value less than one suggested the formation of an inclusion complex with 1:1 stoichiometry.

Considering the tendency of βCD-MEA to aggregate in water, an AL-type linear phase-solubility diagram can be consistent with an equilibrium between aggregates and monomeric 1:1 inclusion complex (Jansook et al., 2010). Within this framework, an apparent stability constant of 1127 M^{-1} was determined for the βCD-MEA/CAR complex. This value is higher than that reported for the βCD/CAR complex (155 M^{-1}, Santos et al., 2015), suggesting that the amino-alcohol substituents shift the equilibrium toward the complex formation. Importantly, this Kc remains within a suitable range for effective CAR release. A higher K_c value (2268.2 M^{-1}) reported for the hydroxypropyl-βCD/CAR inclusion complex was associated with a lower CAR release and diminished antibacterial activity (López-Miranda et al., 2021), indicating that excessively stable complexes may hinder therapeutic efficacy.

From the slope of the phase solubility diagram (Fig. S11), the complexation efficiency (CE) was calculated to be 7.55, indicating that, on average, only about one out of every nine βCD-MEA molecules is empty (Loftsson et al., 2005).

3.2.4. Dimensional and morphological characterization of the βCD-MEA/CAR complex

DLS analysis revealed that the nanosuspension of the βCD-MEA/CAR complex contains nanoaggregates with a mean hydrodynamic diameter of 300 ± 11 nm (Z average) (Fig. 5A), PDI of 0.22 ± 0.01, and a negative Zeta potential value (ζ = −36 ± 1 mV) (Fig. 5B). The size of the βCD-MEA/CAR complex was smaller than that reported for the βCD/CAR complex prepared using the same technique (mean hydrodynamic diameter 899 nm, PDI 0.34) (Santos et al., 2015), The smaller size, likely due to the higher water solubility of βCD-MEA, is advantageous for applications in drug delivery.

AFM image (Fig. 5C) revealed that the complex consists of *quasi*-spherical nanostructures with an average height of 51.3 ± 18.8 nm and width of 97.6 ± 24.9 nm. Upon increasing the concentration from 1 mg to 5 mg/mL, the morphology was preserved, with a slight increase in aggregate size (62.9 ± 25.7 nm average height and 128.3 ± 37.8 nm average width, Fig. S12).

The tendency toward agglomeration was also reported for the βCD/CAR complex, for which TEM images showed larger particles attracting smaller ones (Santos et al., 2015).

3.2.5. Antioxidant activity of the βCD-MEA/CAR complex

The antioxidant activity of the inclusion complex was evaluated using the in vitro DPPH radical scavenging assay, based on a dual mechanism of hydrogen atom transfer and deprotonation/electron transfer (Foti, 2015). Pure CAR was initially tested over a concentration range of 0.8–0.012.5 mg/mL to determine its intrinsic antioxidant potential. The results of the assay showed that CAR exhibited radical scavenging activity starting from the concentration of 0.05 mg/mL, achieving approximately 50 % inhibition of the DPPH radical at a concentration of 0.8 mg/mL (IC_{50} = 0.71 ± 0.04 mg/mL). DPPH experiments indicated that empty βCD-MEA did not possess free radical scavenging properties, whereas the scavenging activity of CAR (0.2 mg/mL) in the complex was 15.97 ± 0.59 %, similarly to CAR alone (15.44 ± 0.49) at the same concentration. Therefore, CAR retains its

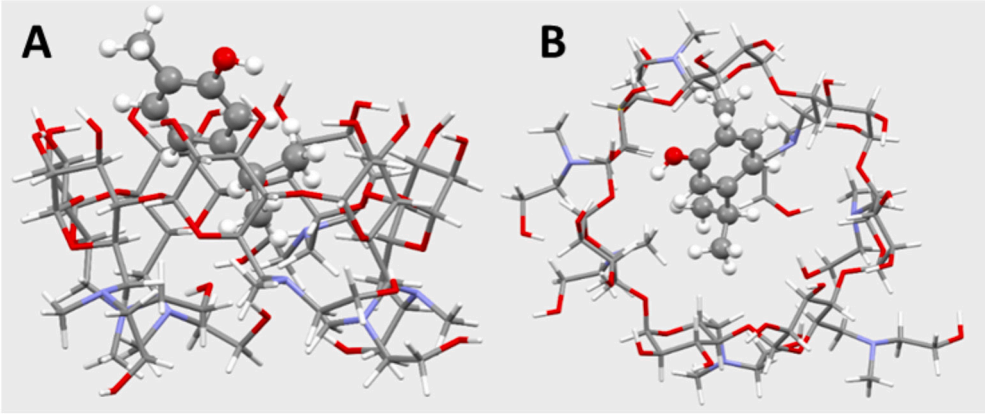

Fig. 4. Structure of the βCD-MEA/CAR complex from computational simulations: A) side view and B) up view.

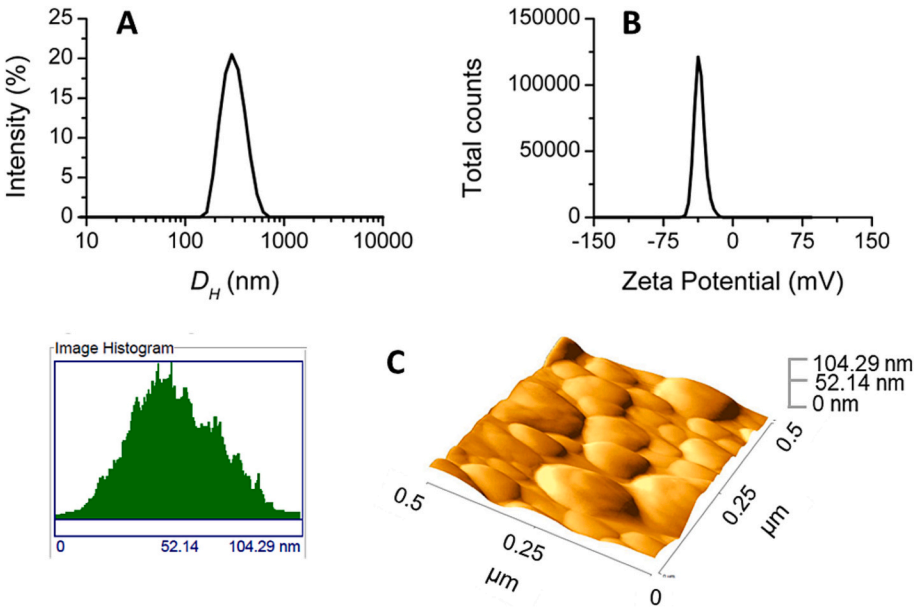

Fig. 5. Characterization of the βCD-MEA/CAR nanoaggregates: A) Intensity weighted distribution of the hydrodynamic diameter; B) Zeta potential distribution; C) Size distribution histogram and representative AFM image of the sample (1 mg/mL in water) on Si substrate, three-dimensional reconstruction.

antioxidant properties in the complex. Literature studies have reported similar findings, with CAR exhibiting comparable or slightly reduced antioxidant activity when complexed with βCD (Santos et al., 2015).

3.3. Microbiological studies

The antibacterial activity of βCD-MEA/CAR, CAR and βCD-MEA was evaluated against both Gram-positive and Gram-negative bacteria (Table 1).

The results demonstrated a similar trend for CAR and βCD-MEA/CAR, with MIC values equal to 0.05–0.1 mg/mL for *S. aureus* and *E. coli*, respectively, whereas no antibacterial activity was detected for βCD-MEA at the highest concentration tested. MBC values were >0.1 mg/mL for both bacteria.

The retention of the antibacterial activity of CAR is a positive result considering that for the hydroxypropyl-βCD/CAR complex, prepared by the freeze-drying method, a reduction in CAR antibacterial activity was reported. In particular, against *E. coli* O157:H7 and *S. aureus* USA300, the MIC was found to be 700 and 150–200 µg/mL for hydroxypropyl-βCD/CAR complex and CAR, respectively (López-Miranda et al., 2021). Nevertheless, in the literature are also present studies reporting an increased antimicrobial activity of CAR when encapsulated in βCD and hydoxypropyl-βCD (Kamimura et al., 2014; Rodríguez-López et al., 2020; Santos et al., 2015).

Biofilms formed by several bacterial strains still pose a significant challenge to healthcare due to their resistance to conventional treatment approaches, including antibiotics. The effect of βCD-MEA/CAR, CAR, and empty βCD-MEA was also evaluated in terms of inhibition of biofilm formation and dissolution of preformed biofilm of *S. aureus* ATCC 6538 (Figs. 6 and 7). Against *S. aureus* biofilm formation (Fig. 6), both βCD-MEA/CAR and CAR showed significant efficacy ($p < 0.05$) at concentrations of 0.5 × MIC (CAR 0.025 mg/mL, βCD-MEA 0.17 mg/mL).

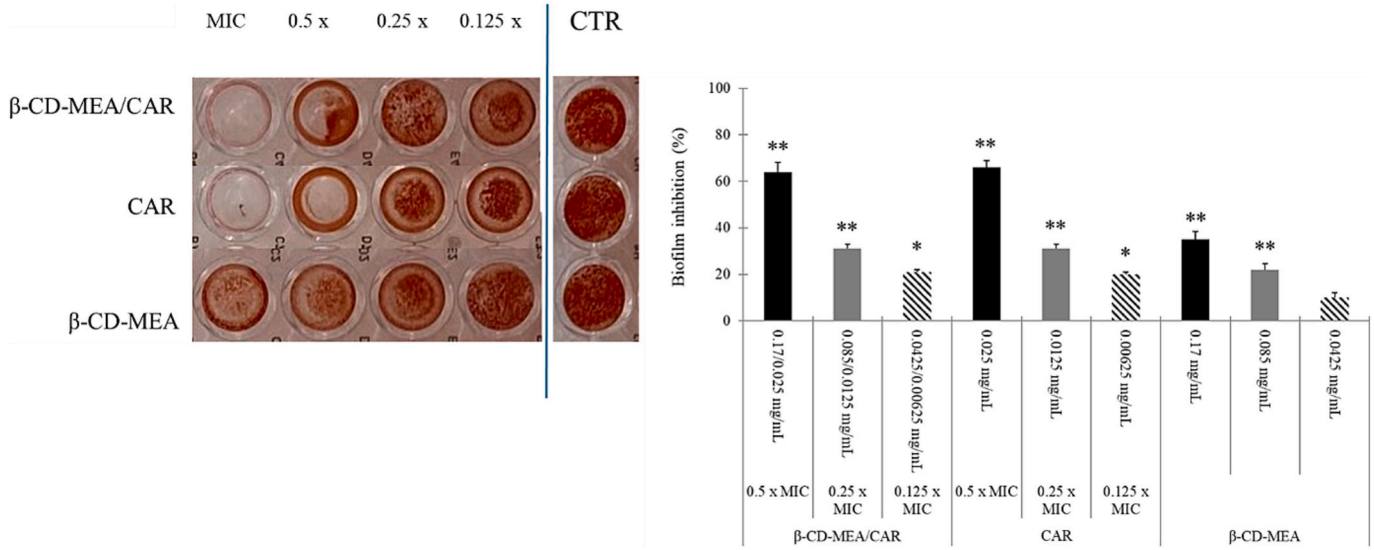

Fig. 6. Effects of different concentrations (from 0.5 to 0.125 × MIC) of βCD-MEA/CAR, CAR, and βCD-MEA on biofilm formation of *S. aureus* ATCC 6538. All data are presented as mean ± SD, the asterisk indicates statistically difference with the positive control (* $p \leq 0.05$; ** $p \leq 0.01$).

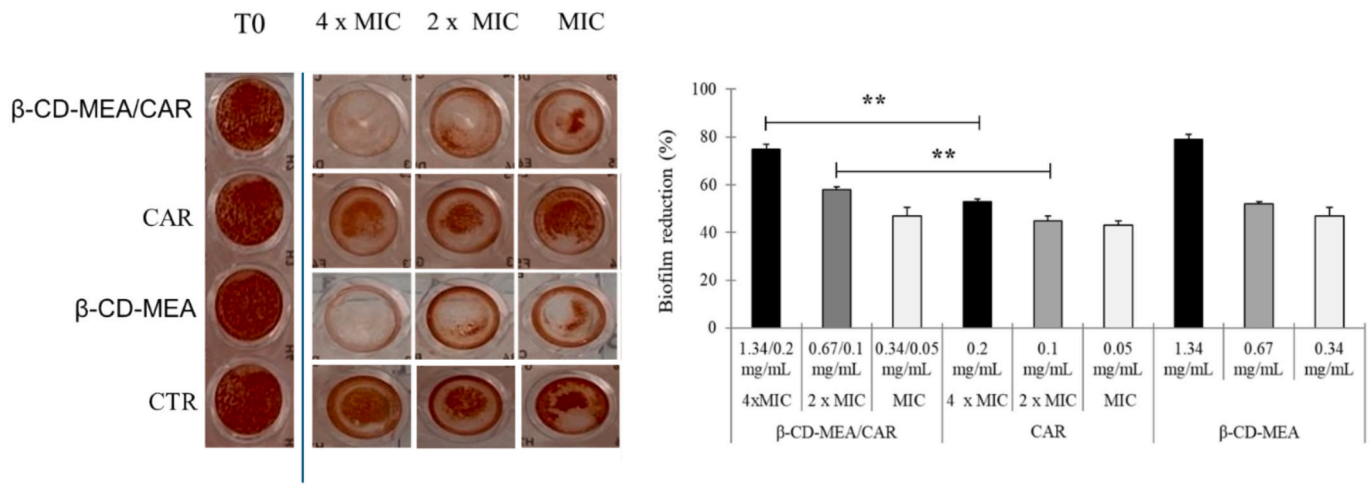

Fig. 7. Effects of different concentrations (from MIC to 4 × MIC) of βCD-MEA/CAR, CAR, and βCD-MEA on 24 h-biofilm of *S. aureus* ATCC 6538. All data are presented as mean ± SD, the asterisk indicates statistical differences (** $p \leq 0.01$).

Specifically, the effective percentage reductions of biofilm formation were 64 % and 66 % respectively. A lower effect (31 %) was observed with 0.25 × MIC (CAR 0.0125 mg and βCD-MEA 0.085 mg/mL). Interestedly, empty βCD-MEA (0.17 and 0.085 mg/mL) also determined a biofilm inhibition equal to 35–22 %.

The samples were also effective against preformed biofilm of *S. aureus*. βCD-MEA/CAR exhibited a significant higher biofilm biomass reduction (75 %, 58 %, 47 %) than CAR (53 %, 45 %, 43 %) at doses equal to 4 × MIC, 2 × MIC, and MIC, corresponding to 1.34, 0.67, and 0.34 mg/mL of βCD-MEA and 0.2, 0.1, and 0.05 mg/mL of CAR, respectively (Fig. 7). Noteworthy, empty βCD-MEA at concentration of 1.34, 0.67, and 0.34 mg/mL showed intrinsic activity with biofilm biomass reductions of 84 %, 52 %, and 47 %, respectively. This behavior suggested possible interactions of the amino-alcohol groups of βCD-MEA with the components of the biofilm matrix. As a support, disruption and dispersion of *Vibrio cholerae* biofilm was reported for quinoline amino alcohols (León et al., 2015).

The dual action of the samples examined is consistent with literature data reporting that an inclusion complex of essential oil with βCD both prevented biofilm formation and disrupted established biofilms (Alabrahim et al., 2025).

4. Conclusions

In this study, a novel water-soluble β-cyclodextrin derivative bearing seven polar methylaminoethanol groups (βCD-MEA) was synthesized and structurally characterized. As hypothesized, the β-cyclodextrin derivative forms water-soluble nanoaggregates, with a quasi-spherical morphology as evidenced by DLS and AFM images. The capability of βCD-MEA to complex a hydrophobic drug as carvacrol was demonstrated by NMR spectroscopy and a phase solubility study. Molecular modelling simulations suggested a structure in which the isopropyl group of carvacrol is oriented toward the cyclodextrin narrow edge. The carvacrol-loaded nanostructures showed slightly increased size and Zeta potential, and unchanged morphology compared to the empty βCD-MEA. The complexed carvacrol retained its radical scavenging, antibacterial, and antibiofilm activities. Noteworthy, βCD-MEA also exhibited no significant toxicity toward *Artemia salina* and showed an intrinsic ability to disrupt preformed biofilm of *S. aureus*. These properties, along with its potential as a nanocarrier for drug delivery, make βCD-MEA a promising candidate in the emerging field of nanobiotics, which integrates nanotechnology and antimicrobial activity to combat pathogenic microorganisms.

CRediT authorship contribution statement

Sonia Pedotti: Methodology, Investigation, Conceptualization. **Giovanna Ginestra:** Methodology, Investigation, Formal analysis. **Giuseppe Granata:** Methodology, Investigation, Formal analysis, Conceptualization. **Loredana Ferreri:** Methodology, Investigation. **Giovanni Gambera:** Methodology, Investigation. **Salvatore Petralia:** Methodology, Investigation. **Francesco Ruffino:** Methodology, Investigation. **Maria Fernanda Taviano:** Methodology, Investigation. **Antonia Nostro:** Writing – original draft, Supervision, Funding acquisition, Conceptualization. **Grazia Maria Letizia Consoli:** Writing – review & editing, Writing – original draft, Supervision, Funding acquisition, Conceptualization.

Funding

This research was funded by the European Union (NextGeneration EU), project PRIN PNRR "Novel biomedical devices combining antimicrobial and anti-inflammatory activity by embedding bioactive loaded nanoconstructs in polymer films for more effectiveness in infectious disease treatment (BIONANOF)" (grant number P20229ZLSA).

Declaration of competing interest

The Authors declare that they have no known competing financial interests or personal relationship that could have appeared to influence the work reported in this paper.

Acknowledgements

We would like to acknowledge Mr. Francesco Mugheddu, Mr. Antonio Greco, and Mr. Agatino Renda (CNR ICB Catania, Italy) for technical assistance.

Appendix A. Supplementary data

1D- and 2D-NMR and ESI-MS spectra of βCD-MEA, FTIR spectra of βCD, βCD-MEA and βCD-MEA/CAR complex, AFM images of βCD-MEA and βCD-MEA/CAR at higher concentration, molecular modelling simulated structure of βCD-MEA/CAR complex, phase solubility curve fitting. Supplementary data to this article can be found online at https://doi.org/10.1016/j.carbpol.2025.124540.

Data availability

Data will be made available on request.

References

Alabrahim, O. A. A., Fytory, M., Abou-Shanab, A. M., Lababidi, J., Fritzsche, W., El-Badri, N., & El-Said Azzazy, H. M. (2025). A biocompatible β-cyclodextrin inclusion complex containing natural extracts: A promising antibiofilm agent. *Nanoscale Advance, 7*, 1405–1420. https://doi.org/10.1039/D4NA00916A

Ates, K., & Yildiz, Z. I. (2025). Encapsulation of carvacrol in β-cyclodextrin metal-organic frameworks: Improved solubility, stability, antioxidant capacity and controlled release of carvacrol. *Journal Of Food Engineering, 391*, Article 112445. https://doi.org/10.1016/j.jfoodeng.2024.112445

Bonini, M., Rossi, S., Karlsson, G., Almgren, M., Lo Nostro, P., & Baglioni, P. (2006). Self-assembly of β-cyclodextrin in water. Part 1: Cryo-TEM and dynamic and static light scattering. *Langmuir, 22*, 1478–1484. https://doi.org/10.1021/la052878f

Cedillo-Flores, O. E., Rodríguez-Laguna, N., Hipólito-Nájera, A. R., Nivón-Ramírez, D., Gómez-Balderas, R., & Moya-Hernández, R. (2022). Effect of the pH on the thermodynamic stability of inclusion complexes of thymol and carvacrol in β-cyclodextrin in water. *Food Hydrocolloids, 124*(Part B), Article 107307. https://doi.org/10.1016/j.foodhyd.2021.107307

Clinical and Laboratory Standards Institute. (2018). *Methods for dilution antimicrobial susceptibility tests for bacteria that grow aerobically: M07-A11* (11th. ed.). Wayne, PA, USA: CLSI.

Consoli, G. M. L., Maugeri, L., Forte, G., Bongiorno, D., Nicitra, E., Aleo, D., Spitaleri, F., Ferreri, L., Buscarino, G., Campagna, T., Musso, N., & Petralia, S. (2025). Bioinspired β-cyclodextrin-derived carbon dots with emissive and photothermal properties as nanocarriers for bioactive agents. *ACS Applied Nano Materials, 8*, 1078–1090. https://doi.org/10.1021/acsanm.4c05858

Dodziuk, H. (2006). Molecules with Holes—Cyclodextrins. In *Cyclodextrins and their complexes* (pp. 1–30). Weinheim, Germany: Wiley-VCH Verlag GmbH & Co. KGaA.

Esteso, M. A., & Romero, C. M. (2024). Cyclodextrins: Properties and applications. *International Journal of Molecular Science, 25*(8), Article 4547. https://doi.org/10.3390/ijms25084547

Fatima, N., Khalid, S. H., Liaqat, K., Zulfiqar, A., & Munir, R. (2023). Beta-cyclodextrin: A cyclodextrin derivative and its various applications. *Polymer Science, 4*(5). https://doi.org/10.31031/PSPRJ.2023.04.000597. PSPRJ. 000597.

Foti, M. C. (2015). Use and abuse of the DPPH(•) radical. *Journal of Agricultural and Food Chemistry, 63*(40), 8765–8776. https://doi.org/10.1021/acs.jafc.5b03839

French, D., Levine, M. L., Pazur, J. H., & Norberg, E. (1949). Studies on the Schardinger dextrins; The preparation and solubility characteristics of alpha, beta and gamma dextrins. *Journal American Chemical Society, 71*, 353. https://doi.org/10.1021/ja01169a100

Gonzalez Pereira, A., Carpena, M., García Oliveira, P., Mejuto, J. C., Prieto, M. A., & Simal Gandara, J. (2021). Main applications of cyclodextrins in the food industry as the compounds of choice to form host–guest complexes. *International Journal of Molecular Sciences, 22*(3), Article 1339. https://doi.org/10.3390/ijms22031339

Granata, G., Accardo, P., Leotta, C. G., Pitari, G. M., Fangano, G., Ruffino, F., … Consoli, G. M. L. (2025). Preparation, characterization and in vitro evaluation of anticancer and antioxidant effects of luteolin-loaded nanocapsules. *Journal of Drug Delivery Science and Technology, 107*, Article 106754. https://doi.org/10.1016/j.jddst.2025.106754

Granata, G., Paterniti, I., Geraci, C., Cunsolo, F., Esposito, E., Cordaro, M., … Consoli, G. M. L. (2017). Potential eye drop based on a calix[4]arene nanoassembly for curcumin delivery: Enhanced drug solubility, stability and anti-inflammatory effect. *Molecular Pharmaceutics, 14*, 1610–1622. https://doi.org/10.1021/acs.molpharmaceut.6b01066

Hamidi, M. R., Jovanova, B., & Panovska, T. K. (2014). Toxicological evaluation of the plant products using brine shrimp (Artemia salina L.) model. *Macedonian. Pharmaceutical Bulletin, 60*(1), 9. https://doi.org/10.33320/maced.pharm.bull.2014.60.01.002

Hbaieb, S., Kalfat, R., Chevalier, Y., Amdouni, N., & Parrot-Lopez, H. (2008). Influence of the substitution of β-cyclodextrins by cationic groups on the complexation of organic anions. *Material Science Engineering C, 28*, 697. https://doi.org/10.1016/j.msec.2007.10.013

Higuchi, T., & Connors, K. A. (1965). Phase solubility techniques. *Advanced Analytical Chemistry of Instrumentation, 4*, 117–212.

Huang, J., Wang, X., Yang, T. H., Tu, J., Zou, J., Yang, H., & Yang, R. (2024). Application of sodium sulfobutylether-β-cyclodextrin based on encapsulation. *Carbohydrates Polymers, 333*, Article 121985. https://doi.org/10.1016/j.carbpol.2024.121985

Jansook, P., Kurkov, S. V., & Loftsson, T. (2010). Cyclodextrins as solubilizers: Formation of complex aggregates. *Journal of Pharmaceutical Sciences, 99*, 719–729. https://doi.org/10.1002/jps.21861

Kamimura, J. A., Santos, E. H., Hill, L. E., & Gomes, C. L. (2014). Antimicrobial and antioxidant activities of carvacrol microencapsulated in hydroxypropyl-beta-cyclodextrin. *LWT–Food Science Technology, 57*, 701–709. https://doi.org/10.1016/j.lwt.2014.02.014

Kfoury, M., Lichtfouse, E., & Fourmentin, S. (2025). The revival of cyclodextrins as active pharmaceutical ingredients. *Environmental Chemistry Letters, 23*, 1–6. https://doi.org/10.1007/s10311-024-01782-8

León, B., Haeckl, F. P., & Linington, R. G. (2015). Optimized quinoline amino alcohols as disruptors and dispersal agents of *Vibrio cholerae* biofilms. *Organic Biomolecular Chemistry, 13*(31), 8495–8499. https://doi.org/10.1039/c5ob01134e

Li, Z., Jiang, X., Zhu, L., Chen, F., Liu, H., & Ming, L. (2022). New insights into the thermal degradation behavior of Hydroxypropyl-beta-cyclodextrin inclusion complexes containing Carvacrol essential oil via thermogravimetric analysis. *Journal of Thermal Analysis and Calorimetry, 147*, Article 11301. https://doi.org/10.1007/s10973-022-11327-2

Libralato, G., Prato, E., Migliore, L., Cicero, A. M., & Manfra, L. (2016). A review of toxicity testing protocols and endpoints with Artemia spp. *Ecological Indicators, 69*, 35. https://doi.org/10.1016/j.ecolind.2016.04.017

Locci, E., Lai, S., Piras, A., Marongiu, B., & Lai, A. (2004). ^{13}C-CPMAS and ^{1}H-NMR study of the inclusion complexes of beta-cyclodextrin with carvacrol, thymol, and eugenol prepared in supercritical carbon dioxide. *Chemistry Biodiversity, 1*(9), 1354–1366. https://doi.org/10.1002/cbdv.200490098

Loftsson, T., Hreinsdóttir, D., & Másson, M. (2005). Evaluation of cyclodextrin solubilization of drugs. *International Journal of Pharmaceutics, 302*, 18–28. https://doi.org/10.1016/j.ijpharm.2005.05.042

Loftsson, T., Hreinsdóttir, D., & Másson, M. (2007). The complexation efficiency. *Journal of Inclusion Phenomena and Macrocyclic Chemistry, 57*, 545–552. https://doi.org/10.1007/s10847-006-9247-2

López-Miranda, S., Berdejo, D., Pagán, E., García-Gonzalo, D., & Pagán, R. (2021). Modified cyclodextrin type and dehydration methods exert a significant effect on the antimicrobial activity of encapsulated carvacrol and thymol. *Journal of the Science of Food and Agriculture, 101*(9), 3827–3835. https://doi.org/10.1002/jsfa.11017

Martina, K., Caporaso, M., Tagliapietra, S., Heropoulos, G., Rosati, O., & Cravotto, G. (2011). Synthesis of water-soluble multidentate aminoalcohol β-cyclodextrin derivatives via epoxide opening. *Carbohydrate Research, 346*(17), 2677–2682. https://doi.org/10.1016/j.carres.2011.09.018

Maugeri, L., Fangano, G., Butera, E., Forte, G., Bonacci, P. G., Musso, N., … Petralia, S. (2025). Emissive pentacene-loaded βcyclodextrin-derived C-nanodots exhibit red-light triggered photothermal effect. *Pharmaceutics, 17*, 543. https://doi.org/10.3390/pharmaceutics17050543

Meyer, B. N., Ferrigni, N. R., Putnam, J. E., Jacobson, L. B., Nichols, D. E., & McLaughlin, J. L. (1982). Brine shrimp: A convenient general bioassay for active plant constituents. *Planta Medica, 45*, 31–34. https://doi.org/10.1055/s-2007-971236

Neves, A. T. F., Stenner, R., Race, P. R., & Curnow, P. (2022). Expression, purification and preliminary characterisation of the choline transporter LicB from opportunistic bacterial pathogens. *Protein Expression and Purification, 190*, Article 106011. https://doi.org/10.1016/j.pep.2021.106011

Nostro, A., Marino, A., Blanco, A. R., Cellini, L., Di Giulio, M., Pizzimenti, F., … Bisignano, G. (2009). In vitro activity of carvacrol against staphylococcal preformed biofilm by liquid and vapour contact. *Journal of Medical Microbiology, 58*, 791. https://doi.org/10.1099/jmm.0.009274-0

Nostro, A., Sudano Roccaro, A. S., Bisignano, G., Marino, A., Cannatelli, M. A., Pizzimenti, F. C., … Blanco, A. R. (2007). Effects of oregano, carvacrol and thymol on *Staphylococcus aureus* and *Staphylococcus epidermidis* biofilms. *Journal of Medical Microbiology, 56*, 519. https://doi.org/10.1099/jmm.0.46804-0

Ohnishi, M., Morishita, H., Iwahashi, H., Toda, S., Shirataki, Y., Kimura, M., & Kido, R. (1994). Inhibitory effects of chlorogenic acid on linoleic acid peroxidation and haemolysis. *Phytochemistry, 36*(3), 579–583. https://doi.org/10.1016/S0031-9422(00)89778-2

Pedotti, S., Ferreri, L., Migliore, R., Leotta, C. G., Pitari, G. M., D'Antona, N., … Consoli, G. M. L. (2024). A novel cationic β-cyclodextrin decorated with a choline-like pendant exhibits iodophor, mucoadhesive and bactericidal properties. *Carbohydrate Polymers, 328*, Article 121698. https://doi.org/10.1016/j.carbpol.2023.121698

Plett, C., & Grimme, S. (2023). Automated and efficient generation of general molecular aggregate structures. *Angewandte Chemie International Edition, 62*, Article e202214477. https://doi.org/10.1002/anie.202214477

Pollit, F. D. (1996). Safety evaluation of certain food additives (β-cyclodextrin). *WHO Food Additives: Series, 54*(35), 257–268.

Puskás, I., Szente, L., Szőcs, L., & Fenyvesi, É. (2023). Recent list of cyclodextrin-containing drug products. *Periodica Polytechnica, Chemical Engineering, 67*, 11–17. https://doi.org/10.3311/PPch.21222

Ri, K., Weng, T.-H., Cabezudo, A. C., Jösting, W., Zhang, Y., Bazzone, A., … Safarian, S. (2024). Molecular mechanism of choline and ethanolamine transport in humans. *Nature, 630*, 501. https://doi.org/10.1038/s41586-024-07444-7

Rodríguez-López, M. A., Mercader-Ros, M. T., Pellicer, J. A., Gómez-López, V., Martínez-Romero, D., Núñez-Delicado, E., & Gabaldón, J. A. (2020). Evaluation of monoterpene-cyclodextrin complexes as bacterial growth effective hurdles. *Food Control, 108*, Article 106814. https://doi.org/10.1016/j.foodcont.2019.106814

Santos, E. H., Kamimura, J. A., Hill, L. E., & Gomes, C. L. (2015). Characterization of Carvacrol beta-cyclodextrin inclusion complexes as delivery systems for antibacterial and antioxidant applications. *LWT - Food Science and Technology, 60*(1), 583–592. https://doi.org/10.1016/j.lwt.2014.08.046

Sharifi-Rad, M., Varoni, E. M., Iriti, M., Martorell, M., Setzer, W. N., Del Mar Contreras, M., … Sharifi-Rad, J. (2018). Carvacrol and human health: A comprehensive review. *Phytotherapy Research, 32*(9), 1675. https://doi.org/10.1002/ptr.6103

Shen, H.-M., & Ji, H.-B. (2012). Amino alcohol-modified b-cyclodextrin inducing biomimetic asymmetric oxidation of thioanisole in water. *Carbohydrate Research, 354*, 49. https://doi.org/10.1016/j.carres.2012.03.034

Singh, P., & Mahar, R. (2024). Cyclodextrin in drug delivery: Exploring scaffolds, properties, and cutting-edge applications. *International Journal of Pharmarmaceutics, 662*, Article 124485. https://doi.org/10.1016/j.ijpharm.2024.124485

Valderrama, A., & Rojas De, G. (2017). Traceability of active compounds of essential oils in antimicrobial food packaging using a chemometric method by ATR-FTIR.

American Journal of Analytical Chemistry, 8, 726–741. https://doi.org/10.4236/ajac.2017.811053

Watanabe, S., Nishijima, N., Hirai, K., Shibata, K., Hase, A., Yamanaka, T., & Inazu, M. (2020). Anticancer activity of Amb4269951, a choline transporter-like protein 1 inhibitor, in human glioma cells. *Pharmaceuticals, 13*, Article 104. https://doi.org/10.3390/ph13050104 (and references therein).

Yu, J., & Lu, Y. (2018). *Artemia* spp. model-a well-established method for rapidly assessing the toxicity on an environmental perspective. *Medical Research Archives, 6* (2), 1–15. https://doi.org/10.18103/mra.v6i2.1700